South African Journal of Chemical Engineering 51 (2025) 86–94

Contents lists available at ScienceDirect

South African Journal of Chemical Engineering

journal homepage: www.elsevier.com/locate/sajce

Bambara groundnut starch-soluble dietary fibre nanocomposite stabilised emulsions: Optimisation of emulsion stability and studies on time-dependent rheological properties

Yvonne Maphosa [a,*], Oladayo Adeyi [b], Daniel Imwansi Ikhu-Omoregbe [c], Victoria A. Jideani [a]

[a] Department of Food Science and Technology, Cape Peninsula University of Technology, P.O. Box 1906, Bellville, Cape Town 7535, South Africa
[b] Department of Chemical Engineering, Michael Okpara University of Agriculture, PMB 7267, Umudike, Abia State, Nigeria
[c] Department of Chemical Engineering, Cape Peninsula University of Technology, P.O. Box 1906, Bellville, Cape Town 7535, South Africa

ARTICLE INFO

Keywords:
Bambara groundnut
Emulsion
Nanocomposite
Optimisation
Rheology
Stability

ABSTRACT

Due to their inherent thermodynamic instability, emulsions require stabilisers to maintain their integrity and prevent destabilisation. The effect of emulsion components (Bambara groundnut starch-soluble dietary fibre nanocomposite (STASOL), orange oil and water) on the rheological and stability properties of STASOL-stabilised emulsions was optimised. A randomised D-optimal exchange mixture design was used to determine the ratio of STASOL, orange oil and water required for a stable emulsion. The stability of these emulsions was evaluated using the initial mean backscattering index (BS_{AVO}), Turbiscan stability index (TSI) and hysteresis loop area (HLA). The BS_{AVO} (%), TSI and HLA of the emulsions ranged from 50.73 % (14:30:56 STASOL:oil:water) to 70.47 % (20:30:50 STASOL:oil:water), 0.0005 (20:30:50 STASOL:oil:water) to 0.1000 (8:42:50 STASOL:oil:water) and 0.37 Pas^{-1} (10:32:58 STASOL:oil:water) to 5.69 Pas^{-1} (20:30:50 STASOL:oil:water), respectively. Emulsions exhibited a direct relationship between STASOL concentration and stability metrics, with the highest stability achieved at 20 % STASOL concentration, 30 % orange oil and 50 % water. An increase in STASOL concentration coupled with a decrease in oil concentration results in a stable emulsion. Numerical optimisation and experimental validation confirmed the effectiveness of the selected formulation, demonstrating STASOL's potential as a natural stabiliser in beverage emulsions and its ability to enhance stability compared to synthetic alternatives.

1. Introduction

Emulsions are complex systems that rely on the composition of the aqueous and oil phases, as well as the use of stabilisers, to maintain their stability (Kupikowska-Stobba et al., 2024; Akbari & Nour, 2018; Maphosa & Jideani, 2018). Stability directly influences product quality, sensory attributes, shelf life and consumer acceptability (Kakran & Antipina, 2014; Arrebola et al., 2021). To achieve stable emulsions, it is essential to optimise key components such as emulsifier concentration, oil-to-water ratio and agitation parameters during emulsification (Trujillo-Cayado et al., 2016; Rahayu et al., 2019).

Experimental design methods like response surface methodology (RSM) and d-optimal design (DOD) facilitate the efficient adjustment of these factors in optimisation studies. Response surface methodology utilises statistical and mathematical techniques to model and optimise properties (Lamidi et al., 2023), while DOD enhances precision by selecting the best experimental conditions for a given model (Huang et al., 2019). A common application of DOD is the D-optimal point exchange mixture design (DOPEMD), which is particularly useful for optimising emulsion formulation in mixture experiments (Rahayu et al., 2019). The stability of emulsions can be assessed using several important descriptors such as backscattering flux, Turbiscan stability index (TSI) and hysteresis loop area (HLA). These metrics are instrumental in optimising formulations and predicting shelf life in colloidal systems (Adeyi et al., 2014a).

Backscattering flux is an optical characterisation method that monitors the physical behaviour of emulsions over time using Turbiscan technology (Maphosa et al., 2023). By analysing changes in backscattering intensity at various depths, changes in structure and stability can be observed (Choi et al., 2014). The TSI provides a dimensionless measure of destabilisation processes within emulsions, suspensions and foams, ranging from 0 to 100. It is calculated based on differences in

* Corresponding author.
E-mail address: maphosay@cput.ac.za (Y. Maphosa).

https://doi.org/10.1016/j.sajce.2024.11.004
Received 21 August 2024; Received in revised form 24 October 2024; Accepted 3 November 2024
Available online 5 November 2024
1026-9185/© 2024 The Authors. Published by Elsevier B.V. on behalf of South African Institution of Chemical Engineers. This is an open access article under the CC BY-NC-ND license (http://creativecommons.org/licenses/by-nc-nd/4.0/).

backscattering or transmission intensity compared to the original sample (Luo et al., 2017). A higher TSI indicates a loss of stability, suggesting a greater risk of phase separation due to larger droplet sizes (Liu et al., 2015; Perez-Mosqueda et al., 2015; Blasi et al., 2023). The HLA describes the relationship between shear rate and shear stress, serving as an indicator of emulsion stability, rheology and shelf life. This metric is calculated by integrating the area within the hysteresis loop, which is directly proportional to the energy consumed during structural breakdown (Fagundes et al., 2018; Ng et al., 2020). The information gathered from HLA analysis is crucial for optimising formulations and predicting shelf life, particularly in industries like food, where unstable emulsions can compromise product quality before reaching consumers (Maphosa et al., 2023).

Rheology is another critical factor in understanding emulsions. Rheological assessments provide insights into the characteristics and stability of emulsions, allowing predictions of their behaviour during processing, distribution and storage (Oliveira & Cunha, 2015). Time-dependent rheological properties such as viscosity, elasticity and thixotropy are particularly important for understanding emulsion stability over time. These properties can change due to factors such as aging, stabiliser concentration and water volume fraction. Rheological behaviour is often described using models like the first-order stress decay with a zero equilibrium stress value and Weltman models (Farahmandfar et al., 2019).

Recent trends indicate a growing preference for natural stabilisers, particularly biopolymers, due to their biodegradability, eco-compatibility, health benefits and non-toxicity (Liu et al., 2015; Yin et al., 2015; Trujillo-Cayado et al., 2016). While previous studies have explored various stabilisers, there is limited research on natural biopolymer stabilisers derived from underutilised sources. This study aims to address this gap by investigating Bambara groundnut (BGN) starch-soluble dietary fibre nanocomposite (STASOL), a biopolymer nanocomposite developed by Maphosa et al. (2022a).

STASOL is a tasteless, odourless, fine white powder composed of BGNS and BGN-SDF at a ratio of 15:1.95 dry weight. Its excellent hydration, oil-binding capacity, solubility and chemical composition make it an effective emulsion stabiliser. Previous studies on STASOL addressed its functional and antioxidant characteristics (Maphosa et al., 2022a), thermal behaviour, morphology and crystallinity (Maphosa et al., 2022b) and the effect of storage time and temperature on the stability and rheological properties of starch-soluble dietary fibre nanocomposite stabilised emulsions (Maphosa et al., 2023).

The aim of this study was to optimise the stability of STASOL-stabilised emulsions by investigating the effects of emulsion components (STASOL, orange oil and water) and their ratios on the rheological and stability properties of the emulsions.

2. Materials and methods

2.1. Source of materials

Cold-pressed orange oil and Bambara groundnut (BGN) seeds were purchased from Puris Natural Aroma Chemicals (South Africa) and TrioTrade (South Africa), respectively. Commercial grade citric acid (≥99.5 %, Food Chemicals Codex (FCC)), potassium sorbate (EMPROVE® ESSENTIAL, ≥99.0 %, FCC), sodium benzoate (EMPROVE® EXPERT, ≥99 %, FCC), hydrogen peroxide (120 v) and ascorbic acid (FCC, FG) were purchased from Sigma-Aldrich, Merck (South Africa).

2.2. Production of starch-soluble dietary fibre nanocomposite

Bambara groundnut (BGN) starch-soluble dietary fibre nanocomposite (STASOL) has an average particle size of 74.01 nm and exhibits irregular and polygonal morphologies (Maphosa et al., 2022b). It is synthesised by chemically complexing BGN starch and its soluble dietary fibre (SDF) (Maphosa et al., 2022a).

In a 100 mL Schott bottle, deionised water (37.5 mL), BGN starch (BGNS) (15 g), H_2O_2 (120 v) (16.5 %) and ascorbic acid (0.1 %) were incubated at 90 °C for 45 min in a temperature-controlled water bath (Ecobath, LaboTec, South Africa). Following incubation, the solution was cooled and then precipitated for 10 min with absolute ethanol (40 mL) in a sonicator (Sonicator Heat Systems-Ultrasonics, Inc., Model W-225R, Krugersdorp, South Africa) before centrifuging for 5 min at 6 000 rpm (Jouan MR1812 Thermo Electron Corporation). The supernatant was discarded and the residue was rinsed three times with 40 mL of absolute ethanol.

Separately, BGNS (15 g) was dissolved in 40 mL of water:ethanol (1:1 v/v) and BGN-SDF (1.95 g) was dissolved in 15 mL of water:ethanol (1:1 v/v). The two mixtures were then combined and the resulting mixture was stirred on a magnetic stirrer for 24 h (Dragon Lab, MS-H-Pro) in a dark fumehood. The resulting product, STASOL, was freeze-dried (VirTis Genesis 25EL pilot lyophilizer; SP Industries Inc, Warminster, PA, USA), finely ground and stored in ziplock bags.

2.3. Preparation of beverage emulsions

The preparation of beverage emulsions followed the procedure outlined by Maphosa et al. (2017). Specific quantities of STASOL, orange oil and water for each formulation are presented in Table 1. To prevent lumps, STASOL was gradually added to deionised water (60 °C) using a Waring blender and blended for 2 min. Subsequently, orange oil was added, and the mixture underwent further blending at high speed for an additional 2 min. The resulting mixture was homogenised for 5 min at 12,000 rpm using an Ultra Turrax homogeniser (IKA T25 digital, Janke and Kunkel, Staufen, Germany).

2.4. Effects of emulsion components and concentrations on emulsion stability parameters

A randomised d-optimal point exchange mixture design (DOPEMD) was used to determine the amount of the independent variables; STASOL, orange oil and water, required in the formulation of a stable emulsion. Eleven emulsion formulations were prepared and the experimental design is presented in Table 1.

Empirical models were formulated as a function of emulsion components and were employed to predict the optimal combination of STASOL, orange oil and water for achieving a stable emulsion, utilising Design-Expert 9. The measured emulsion stability parameters (response parameters) for each formulation were the initial mean backscattering index (BS_{AVO} (%)), Turbiscan stability index (TSI) and hysteresis loop area (HLA (Pas^{-1})).

Initial backscattering profiles provide insights into the microstructure of freshly prepared emulsions. The BS_{AVO} (%) of the emulsions was determined according to Section 2.6.1. The TSI, a parameter closely related to BS_{AVO} (%), serves as an indicator of emulsion characteristics

Table 1
Randomised D-optimal point exchange mixture design for STASOL* stabilised emulsion.

Formulation	STASOL (%)	Orange oil (%)	Water (%)
1	8	42	50
2	20	30	50
3	8	36	56
4	10	38	62
5	8	42	50
6	8	30	62
7	10	32	58
8	14	30	56
9	14	36	50
10	12	34	54
11	20	30	50

* STASOL: Bambara groundnut starch-soluble dietary fibre nanocomposite.

based on particle size distribution over time, and was determined according to Section 2.6.2.

The HLA is a time-dependent rheological property determined by measuring the energy required to break up an emulsion in comparison to the energy needed for emulsion formation. The HLA was quantified according to Section 2.7.1. The relationship between the response variables (BS_{AVO} (%), TSI and HLA (Pas^{-1})) and all emulsion components (STASOL, orange oil and water) were established using the DOPEMD. All investigated response parameters were thereafter fitted to a second order model presented in Eq. (1) (Oke et al., 2023). The variable Y in Eq. (1) represents the investigated response parameter (BS_{AVO}, TSI or HLA). The constant term in Eq. (1) is β_o; the linear coefficient is β_i; the quadratic coefficient is β_2 and the interactive coefficient is β_3. The Design-Expert software was utilised to determine all the model coefficients, with X_1, X_2 and X_3 representing the coded process parameters. The significance of all regressed model coefficients was statistically determined at confidence level of 95 % using the analysis of variance (ANOVA) test.

$$Y = \beta_1 X_1 + \beta_2 X_2 + \beta_3 X_3 + \beta_{12} X_1 X_2 + \beta_{13} X_1 X_3 + \beta_{23} X_2 X_3 \quad (1)$$

Where: Y = estimated parameters response; β = equation coefficients; X_1, X_2 and X_3 = emulsion components (STASOL, orange oil and water, respectively). $X_1 \times_2$ = interaction between STASOL and orange oil, $X_1 \times_3$ = interaction between STASOL and water and $X_2 \times_3$ = interaction between orange oil and water.

The model adequacies were measured by the R^2(Eq. (2)), R^2_{adj} (Eq. (3)) and Pred R^2 (Eq. (4)) (Oke et al., 2023; Alanzi et al., 2024).

$$R^2 = 1 - \frac{SS_{residual}}{SS_{model} + SS_{residual}} \quad (2)$$

$$R^2_{adj} = 1 - \frac{SS_{residual}/DF_{rediduals}}{SS_{model} + SS_{residual}/DF_{model} + DF_{residual}} \quad (3)$$

$$Pred.\ R^2 = 1 - \frac{PRESS}{SS_{Total}} \quad (4)$$

In equations 2 - 4, the $SS_{residual}$ is the residual sum of squares, SS_{model} is model sum of squares, $DF_{residual}$ is residual degree of freedom, DF_{model} is model degree of freedom, PRESS is predicted residual sum of squares and SS_{Total} is the total sum of squares.

2.5. Numerical optimisation and validation

Simultaneous optimisation of emulsion components and stability, along with rheological parameters, was accomplished using the numerical optimisation algorithm in Design-Expert software, as outlined by Oke et al. (2023). The criteria for optimisation were manually selected in the software's numerical optimiser. The optimisation goal, weight and importance of all variables and responses are presented in Table 2. All suggested optimisation emulsions were ranked based on their desirability values. Furthermore, a validation experiment was carried out to confirm the suggested optimal solution. The statistical parameter employed to compare the predicted and laboratory-validated results was relative standard deviation (RSD). Any RSD greater than 10 between the experimental and suggested optimal response variables was considered similar (Adeyi et al., 2022).

Table 2
Emulsion component and response variables optimisation goal and importance.

Name	Goal	Lower limit	Upper limit	Lower weight	Upper weight	Importance
STASOL (%)	Is in range	8	20	1	1	3
Orange oil (%)	Is in range	30	42	1	1	3
Water (%)	Is in range	50	62	1	1	3
BS_{avo} (%)	Maximise	51.31	70.17	1	1	3
TSI	Minimize	0.0005	0.1	1	1	3
HLA (Pas^{-1})	Maximise	0.4	5.64	1	1	3

STASOL: Bambara groundnut starch-soluble dietary fibre nanocomposite; BS_{Avo}: Initial mean backscattering; TSI: Turbiscan stability index; HLA: Hysteresis loop area.

The RSD was computed using Eq. (5) (Alanzi et al., 2024).

$$\%\ RSD = \frac{SD_{1-2}}{M_v} * 100 \quad (5)$$

Here, SD_{1-2} represents standard deviation and M_v is the mean value of the model predicted and experimental laboratory values.

2.6. Emulsion stability evaluation

Emulsion stability was measured using the optical characterisation method which measures backscattering flux using the Turbiscan (MA 2000, Formulaction, Toulouse, France) (Maphosa et al., 2023), as well as the physical stability method of Perez-Mosqueda et al. (2015) which measures TSI. Each emulsion (7 mL) was measured into a Turbiscan tube (65 mm length) and scanned along its height at 10 min intervals for 60 min. The resulting curves depicted the backscattering and transmission flux percentages relative to the instrument's internal standard across the sample height. To ascertain stability or instability, multiple scans were conducted.

2.6.1. Initial backscattering

The initial backscattering (BS_{AVO}) and transmission curves generated during scanning provided data on the BS_{AVO} and transmission flux relative to the Turbiscan's internal standard as a function of the height of the sample in the tube (Adeyi et al., 2014a). The BS_{AVO} values represented the initial scan of an emulsion immediately after production (Liu et al., 2024).

2.6.2. Turbiscan stability index

The physical stability of emulsions was described using the TSI calculated from Turbiscan analysis data. The TSI, which quantifies destabilisation processes in an emulsion, was calculated using Eq. (6) (Blasi et al., 2023). The TSI is a relative number calculated from the differences in the rate of backscattering or transmission intensity of the sample compared to the original (Luo et al., 2017). It is negatively related to emulsion stability, therefore high values indicate unstable systems (Liu et al., 2015).

$$TSI = \sqrt{\frac{\sum_{i=1}^{n} \left(x_i - x_{BS}\right)^2}{n-1}} \quad (6)$$

Where: TSI = Turbiscan stability index; $\sum$ = sum of all the scan differences from the bottom to the top of the Turbiscan tube; x_i = average value of the scattered light intensity at each time; x_{BS} = average of x_i ; n = number of scans.

2.7. Rheological measurements of emulsions

The rheological characteristics of the STASOL-stabilised emulsions were assessed at 20 °C following the methods described by Adeyi et al. (2014b), using an MCR 300 Paar physical rheometer (Discovery HR-1).

2.7.1. Time-dependent rheological measurements

A 25 mL emulsion sample was transferred to the rheometer cup and allowed to sit for 5 min at room temperature. Subsequently, the emulsion was subjected to an increasing shear rate (0.01–1000 s^{-1}) followed by a decreasing shear rate (1000–0.01 s^{-1}). Information regarding the variation in viscosity over time was collected. The collected data were then fitted to both the first-order stress decay model with a zero equilibrium stress value (Eq. (7)) and the Weltman model (Eq. (8)) (Farahmandfar et al., 2019).

$$\tau = \tau_o e^{-kt} \quad (7)$$

$$\tau = A + B \ln(t) \quad (8)$$

Where: τ = shear stress; t = shearing time; τ_o = initial shear stress value; k = breakdown rate constant. A and B are constants representing the initial shear stress and the time coefficient of thixotropic breakdown, respectively.

A negative B value indicates the rate at which shear stress decreases from the initial value to the final equilibrium (Farahmandfar et al., 2019).

The HLA experiment was conducted in two stages. The initial stage calculated the area between the ascending and descending data curves (Eq. (9)) (Adeyi et al., 2016) and the second stage subjected the emulsions to shear for 20 min at 20 °C, maintaining a constant shear rate of 50, 100 and 150 s^{-1}. Subsequently, the viscosity of the emulsions was measured as a function of shearing time.

$$\int_{\gamma_1}^{\gamma_2} K\gamma^{n} - \int_{\gamma_1}^{\gamma_2} K'\gamma^{n'} \quad (9)$$

Where: K and K$'$ = consistency coefficients and n and n' = flow behaviour indices for upward and downward measurements, respectively.

2.8. Data analysis

All optimisation experiments were conducted in triplicate and the data was presented as mean ± standard deviation. The results were subjected to multivariate analysis of variance (MANOVA) to detect variations in means among different treatments. Duncan's multiple range tests were performed to differentiate means in cases of significant differences (IBM SPSS version 23, 2016). To describe and predict the behaviour of STASOL-stabilised emulsions, rheological modelling was carried out using the MatLab software (2017). The goodness-of-fit of the models was assessed using the coefficient of determination (R^2).

3. Results and discussion

3.1. Model fittings, statistical analysis and adequacies for STASOL, orange oil and water on STASOL-stabilised emulsions

The DOPEMD was used to investigate the effects of STASOL (8–20 %), orange oil (30–42 %) and water (50–62 %) on BS_{AVO} (%), TSI and HLA (Pas^{-1}). The d-optimal design (Table 1) produced 11 experimental runs and was adopted for the construction of predictive models and optimisation of emulsion components for a stable emulsion. The BS_{AVO}, TSI and HLA of STASOL-stabilised emulsions ranged from 50.73 to 70.47 %, 0.0005–0.1000 and 0.37–5.69 Pas^{-1}, respectively (Table 3). Experimental run 11, formulated with the highest amount of STASOL (20 %), lowest amount of orange oil (30 %) and lowest amount of water (50 %), had the highest BS_{AVO} (70.47 %) indicating high initial stability after homogenisation and lowest TSI (0.0005) suggesting a low probability of phase separation. High BS_{AVO} and low TSI values of emulsions indicate high stability (Perez-Mosqueda et al., 2015). The highest stability of experimental run 11 could be attributed to the presence of a higher concentration of STASOL molecules within the emulsion, leading to the formation of a more robust network, and subsequently a more viscous system.

The increased viscosity of the system would impede the movement and subsequent coalescing and/or aggregation of oil droplets (Zhang, 2020; Li et al., 2024). Zalewska et al. (2019) reported a significant decrease in TSI when emulsifier concentration was increased from 5 to 15 % in a plant-based dispersion. As such, it was deduced that an increase in emulsifier or stabiliser concentration in an emulsion decreases the TSI, thereby increasing stability.

Table 3
Effect of STASOL, orange oil and water fractions on BS_{AVO}, TSI and HLA of STASOL-stabilised emulsions.

	Emulsion components			Response values		
Run	STASOL (%)	Orange oil (%)	Water (%)	BS_{AVO} (%)	TSI	HLA (Pas^{-1})
1	8	42	50	66.39 ± 1.51^{ab}	0.0943 ± 0.04^{a}	4.11 ± 0.00^{bc}
2	20	30	50	70.17 ± 4.18^{a}	0.0030 ± 0.02^{b}	5.69 ± 2.36^{bc}
3	8	36	56	59.12 ± 3.25^{c}	0.0243 ± 0.01^{c}	5.20 ± 0.53^{bc}
4	10	38	62	51.31 ± 5.35^{d}	0.0136 ± 0.04^{d}	5.64 ± 1.39^{bc}
5	8	42	50	63.57 ± 2.23^{bc}	0.1000 ± 0.06^{a}	3.32 ± 0.03^{d}
6	8	30	62	55.62 ± 3.21^{d}	0.0402 ± 0.29^{e}	3.88 ± 0.38^{bc}
7	10	32	58	69.11 ± 1.29^{a}	0.0030 ± 0.02^{b}	0.37 ± 0.01^{bc}
8	14	30	56	50.73 ± 1.36^{d}	0.0136 ± 0.04^{d}	0.40 ± 0.12^{a}
9	14	36	50	68.90 ± 1.42^{ac}	0.0207 ± 0.04^{c}	1.50 ± 0.57^{a}
10	12	34	54	58.36 ± 0.49^{c}	0.0245 ± 0.02^{c}	2.04 ± 0.17^{ac}
11	20	30	50	70.47 ± 1.27^{a}	0.0005 ± 0.01^{f}	0.98 ± 0.04^{b}

STASOL: Bambara groundnut starch-soluble dietary fibre nanocomposite; BS_{AVO}: Initial backscattering; TSI: Turbiscan stability index; HLA: Hysteresis loop area. Values are mean ± standard deviation. Means within a column followed by different superscripts are significantly ($p \leq 0.05$) different.

The presence of areas between the backward and forward sweeps (HLA) suggested that all emulsions were time-dependent and thixotropic in nature. A large area between the forward and backward sweeps indicates more extensive damage in the structure of a stabiliser (Junqueira et al., 2018) as was observed in time-dependent studies of infant purees (Alvarez, 2013) and dairy desserts (Tarrega et al., 2004).

3.2. Modelling of process variables for STASOL-stabilised emulsions

The quadratic models that defined the dependence between the studied process parameters and responses in coded terms, obtained with the assistance of RSM, for BS_{AVO}, TSI and HLA are as presented in Eqs. (11)-(13) (Adeyi et al., 2016), respectively.

$$BS_{AVO} = -5.19X_1 + 3.20X_2 - 14.92X_3 + 1.16X_1X_2 - 13.21X_1X_3 - 2.90X_2X_3 \quad (11)$$

$$TSI = -0.003946X_1 + 0.006754X_2 - 0.003353X_3 - 0.026X_1X_2 + 0.005474X_1X_3 - 0.032BX_3 \quad (12)$$

$$HLA = -3.7X_1 + 0.55X_2 - 0.67X_3 - 2.08X_1X_2 - 3.19X_1X_3 + 0.98X_2X_3 \quad (13)$$

Where: X_1, X_2 and X_3 = STASOL, orange oil and water, respectively. The positive (+) and negative (-) signs indicate an increase and a decrease in the response values, respectively, as the process parameters increase.

All linear effects (STASOL, orange oil and water) were significant in the BS_{AVO} model meaning an increase in all the emulsion components resulted in an increase in BS_{AVO}, TSI and HLA. Only the interactive effects of STASOL x water and orange oil x water were significant ($p < 0.05$). All linear effects were insignificant ($p > 0.05$) for the TSI model and the interactive effects of STASOL x orange oil and orange oil and water were significant ($p < 0.05$). Only the effect of water was insignificant in the HLA model and the interactive effects of all emulsion components (STASOL x orange oil, STASOL x water and orange oil x water) were significant ($p < 0.05$).

The ANOVA results for the constructed models, the model coefficients and parameters for measuring model adequacies are presented in Table 4. All the developed response models (Eqs. (11)-(13)) possessed significant (p values < 0.0001) model F-values (BS_{AVO} = 450.22, TSI = 37.88 and HLA = 43.66), insignificant lack of fit values (BS_{AVO} = 0.096, TSI = 9.87 and HLA = 2.37), high R^2 (BS_{AVO} = 0.9985, TSI = 0.9827 and HLA = 0.9850) and high adjusted R^2 (BS_{AVO} = 0.9963, TSI = 0.9568 and HLA = 0.9624) indicating a good fit for the model. Furthermore, the adequate precision of the models were 53.799, 16.484 and 22.868 for BS_{AVO}, TSI and HLA, respectively. Adequate precision is determined by the signal-to-noise ratio, with a ratio exceeding 4 considered desirable. The adequate precision of all models indicated an adequate signal, therefore accepting the applied model in navigating the design space.

Figs. 1, 2 and 3 depict the mixture response surface graphs illustrating the individual and interactive effect of STASOL x orange oil, STASOL x water and water x orange oil on the BS_{AVO}, TSI and HLA of STASOL-stabilised emulsions, respectively. A decrease in orange oil coupled with an increase in STASOL resulted in an increase in BS_{AVO}. Water and STASOL had an antagonistic effect, with a decrease in water and an increase in STASOL resulting in an increase in BS_{AVO}. Orange oil and water showed synergy, with an increase in both resulting in an increase in TSI and HLA of STASOL-stabilised emulsions. Both orange oil and water showed antagonism to STASOL meaning a decrease in STASOL concentration coupled with an increase in both water and orange oil concentrations would result in an unstable emulsion. This indicated decreasing stability with decreasing stabiliser concentration as well as with increasing oil and water concentrations.

3.3. *Numerical optimisation of process variables for STASOL-stabilised emulsions*

The numerical optimisation function within Design Expert software, version 7.0.0 (Stat-Ease, Inc.), was utilised to optimise the stability parameters of emulsions composed of STASOL. The optimisation endeavour pursued a multifaceted set of objectives, which entailed identifying the most favourable composition of emulsion constituents, encompassing STASOL (8–20 %), orange oil (30–42 %) and water (50–62 %), with the dual purpose of maximising BS_{AVO} (%) and HLA (Pas^{-1}), while simultaneously minimising TSI. Each variable, both processing and response, was manually assigned weight (lower and upper bounds) and importance values of 1 and 3, respectively. The selection of the best emulsion composition was based on desirability values, facilitated by the Design Expert software's built-in desirability algorithm. This algorithm integrates individual desirability functions to generate a composite score, enabling the identification of optimal conditions across multiple factors simultaneously. In practical terms, the combined desirability (CD) value serves as a unified metric, summarising the system's performance across various objectives or responses.

Table 5 provides a concise overview of the solutions proposed during the optimisation process aimed at enhancing the stability of emulsions stabilised by STASOL, utilising combined desirability values as the guiding metric. Each of the eleven solutions had a distinct combination of emulsion components and corresponding CD values ranging from 0.512 to 0.823.

Table 4
ANOVA for BS_{AVO}, TSI and HLA quadratic models.

	Source	DF	Sum of squares	Mean square	F-value	Prob > *F*
BS_{AVO}	Model	6	522.47	87.08	450.22	< 0.0001
	A	1	7.16	7.16	37.00	0.0037
	B	1	7.46	7.46	38.57	0.0034
	C	1	186.77	186.77	965.67	< 0.0001
	AB	1	1.23	1.23	6.36	0.0653
	AC	1	149.54	149.54	773.14	< 0.0001
	BC	1	7.21	7.21	37.26	0.0036
	Residual	0.77		4	0.19	
	Lack of Fit	0.19		2	0.096	0.33
	Pure Error	0.58		2	0.29	0.33
	Cor Total	523.24		10		
	R^2	0.9985				
	Adj R^2	0.9963				
	Adequate precision	53.799				
TSI	Model	6	0.012	1.994E-003	37.88	0.0018
	A	1	4.131E-006	4.131E-006	0.078	0.7933
	B	1	3.331E-005	3.331E-005	0.63	0.4709
	C	1	9.438E-006	9.438E-006	0.18	0.6938
	AB	1	5.945E-004	5.945E-004	11.29	0.0283
	AC	1	2.568E-005	2.568E-005	0.49	0.5234
	BC	1	8.517E-004	8.517E-004	16.18	0.0158
	Residual	4	2.105E-004	5.264E-005		
	Lack of Fit	2	1.912E-004	9.559E-005	9.87	0.0920
	Pure Error	2	1.937E-005	9.685E-006		
	Cor Total	10	0.012			
	R^2	0.9827				
	Adj R^2	0.9568				
	Adequate precision	16.484				
HLA	Model	6	23.36	3.89	43.66	0.0013
	A	1	3.62	3.62	40.64	0.0031
	B	1	0.22	0.22	2.51	0.1881
	C	1	0.38	0.38	4.24	0.1085
	AB	1	3.94	3.94	44.23	0.0027
	AC	1	8.74	8.74	98.01	0.0006
	BC	1	0.82	0.82	9.16	0.0389
	Residual	4	0.36	0.089		
	Lack of Fit	2	0.25	0.13	2.37	0.2966
	Pure Error	2	0.11	0.053		
	Cor Total	10	23.72			
	R^2	0.9850				
	Adj R^2	0.9624				
	Adequate precision	22.868				

ANOVA: Analysis of variance. A: STASOL. B: Orange oil. C: Water. Cor Total: Correlation total. R^2: coefficient of determination. Adj R^2: Adjusted coefficient of determination. STASOL: Bambara groundnut starch-soluble dietary fibre nanocomposite. BS_{AVO}: Backscattering index. TSI: Turbiscan stability index. HLA: Hysteresis loop area.

Notably, the least favourable solution (Run 11) with a CD of 0.512 comprised of STASOL (12.16 %), orange oil (36.14 %) and water (50.00 %), predicting BS_{AVO} (66.705 %), TSI (0.028) and HLA (1.577 Pas^{-1}). Conversely, solution number one (Run 1) emerged as the optimal choice due to its highest CD value of 0.823. This leading solution was made of STASOL (20 %), orange oil (30 %) and water (50 %), with predicted BS_{AVO} (69.796 %), TSI (0.002) and HLA (3.417 Pas^{-1}). The CD value of 0.823 for Run 1 aligns closely with the findings of Oke et al. (2023) and

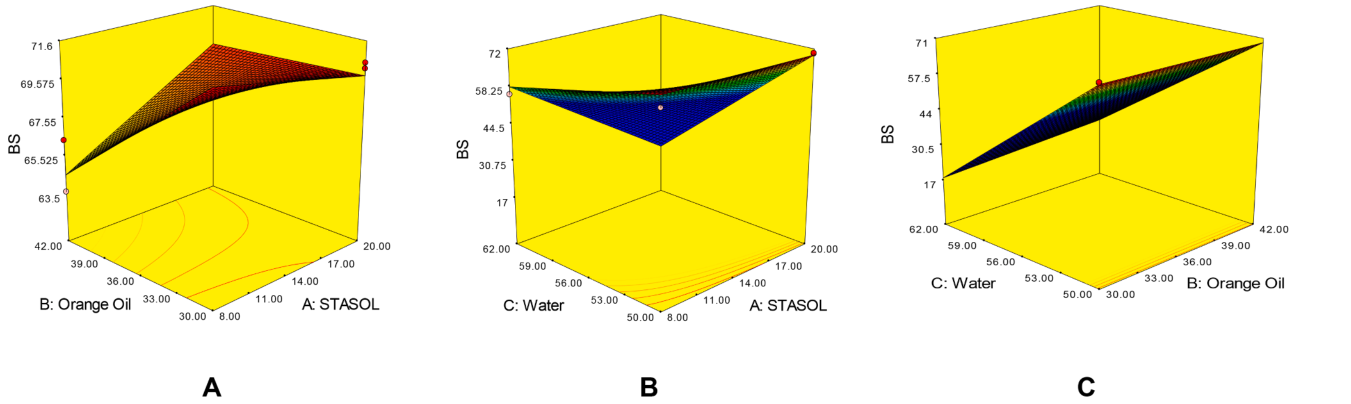

Fig. 1. Effect of (A) STASOL x orange oil, (B) STASOL x water and (C) water x orange oil on the backscattering flux of STASOL-stabilised emulsions. STASOL: Bambara groundnut starch-soluble dietary fibre nanocomposite.

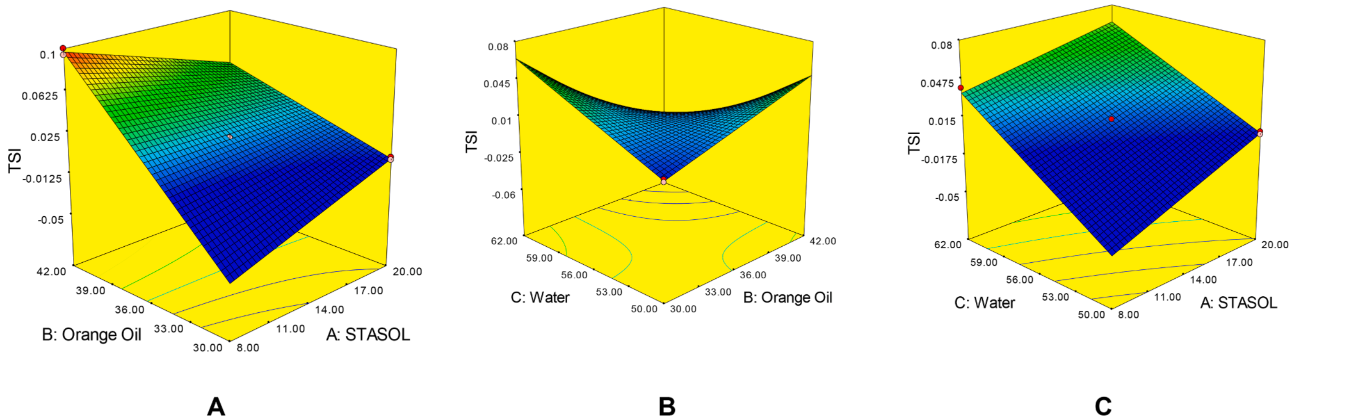

Fig. 2. Effect of (A) STASOL x orange oil, (B) STASOL x water and (C) water x orange oil on the TSI of STASOL-stabilised emulsions. STASOL: Bambara groundnut starch-soluble dietary fibre nanocomposite. TSI: Turbiscan stability index.

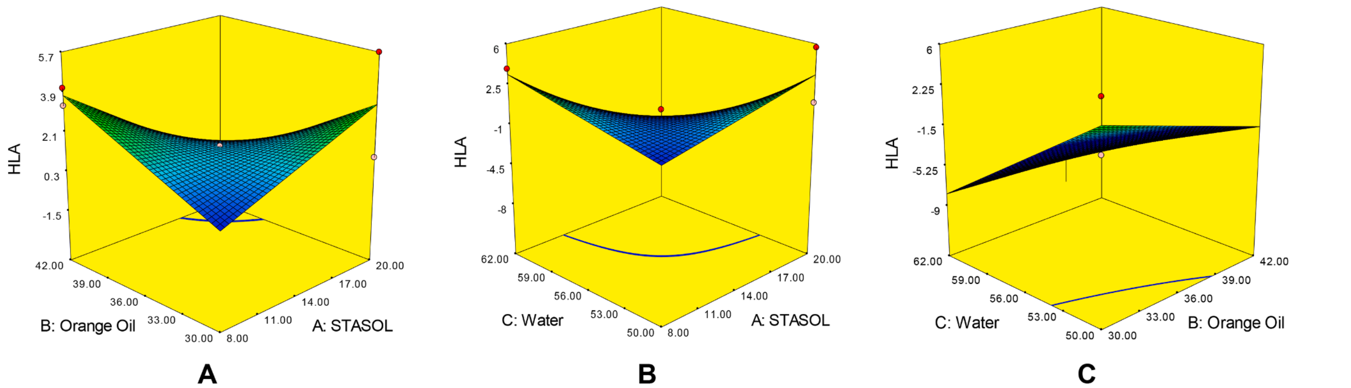

Fig. 3. Effect of (A) STASOL x orange oil, (B) STASOL x water and (C) water x orange oil on the HLA of STASOL-stabilised emulsions. STASOL: Bambara groundnut starch-soluble dietary fibre nanocomposite. HLA: Hysteresis loop area.

Adeyi et al. (2022), reflecting its robustness and efficacy.

After the optimisation process, a validation experiment was conducted in the laboratory to verify the predicted optimal conditions. This involved measuring 20 % STASOL, 30 % orange oil and 50 % water into a beaker, followed by blending for 2 min and homogenising for 5 min at 12,000 rpm using an Ultra Turrax homogeniser. The BS_{AVO}, TSI, and HLA were then quantified according to outlined protocols. The validation experiment yielded the following results: $BS_{AVO} = 68.135$ %, TSI = 0.002 and HLA = 3.316 Pas^{-1}. To assess the consistency between experimental validation and predicted responses, the relative standard deviation (RSD) was calculated. The RSD values for validated and predicted BS_{AVO}, TSI and HLA were found to be 1.70, 4.22 and 2.12 %, respectively, all falling below the 10 % threshold suggested by Adeyi et al. (2022). This concordance underscores the reliability and predictive accuracy of the developed DOPEMD-based models for BS_{AVO}, TSI, and HLA.

3.4. Time-dependent rheological properties

3.4.1. Effect of constant shear decay on apparent viscosity of STASOL-stabilised emulsions

Fig. 4 shows the effect of shearing time on the apparent viscosity of

Table 5
Numerical optimisation solutions.

Number	STASOL (%)	Orange Oil (%)	Water (%)	BS_{AVO} (%)	TSI	HLA (Pas^{-1})	Desirability
1*	20.00	30.00	50	69.7963	0.00172476	3.41682	0.823
2	20.00	30.00	50.56	67.4298	0.0048797	2.96183	0.738
3	16.97	30.00	50:00	66.3283	- 0.006414	2.61899	0.698
4	8.00	36.03	58:81	58.5144	0.0206637	5.64	0.684
5	8.00	36.07	58:76	58.5349	0.0206637	5.63997	0.684
6	8.00	36.12	58:71	58.5556	0.0208768	5.63971	0.684
7	8.00	36.18	58:63	58.5873	0.0212036	5.64004	0.684
8	8.00	35.81	59.09	58.4146	0.0194416	5.64004	0.684
9	8.10	36.96	57.91	58.7985	0.0251562	5.64006	0.678
10	8.00	34.92	58:53	58.4444	0.0173683	4.95995	0.659
11	12.16	36.14	50:00	66.7046	0.0278802	1.57745	0.512

* Selected optimal emulsion. STASOL: Bambara groundnut starch-soluble dietary fibre nanocomposite. BS_{AVO}: Initial backscattering. TSI: Turbiscan stability index. HLA: Hysteresis loop area.

STASOL-stabilised emulsions. All emulsions exhibited time-dependent, shear thinning behaviour when a constant shear rate was applied. Increasing shear rate results in an accelerated breakdown of stabilisers, leading to a reduction in system viscosity and consequently, facilitating droplet movement (Kupikowska-Stobba et al., 2024). When shear is applied over time, the structures of oil droplets and stabilisers are destroyed and coalescence is promoted thereby reducing the resistance of the system to flow (Chen et al., 2023). The behavioural pattern observed in this study was also reported by Junqueira et al. (2018) who described a decrease in viscosity of hydrocolloid-stabilised emulsion systems with increasing shearing time. All STASOL-stabilised emulsions were concluded to be thixotropic. Thixotropic systems exhibit a decrease in viscosity with time when shear is applied to a system previously at rest (Ghica et al., 2016; Schilling & Schmid, 2024). This is common in systems stabilised with hydrocolloids such as galactomannans and xanthan gum (Schilling & Schmid, 2024).

1 = 8:42:50. 2 = 20:30:50. 3 = 8:36:56. 4 = 10:38:62. 5 = 8:42:50. 6 = 8:30:62. 7 = 10:32:58. 8 = 14:30:56. 9 = 14:36:50. 10 = 12:34:54. 11 = 20:30:50 (STASOL:oil:water).

3.4.2. Time-dependent rheological models

The data of the time-dependent behaviour of STASOL-stabilised emulsions were described using the first-order stress decay with a zero equilibrium stress value model (Eq. (7)) and the Weltman model (Eq. (8)).

3.4.2.1. First-order stress decay with a zero equilibrium stress value. The parameters of the first-order stress decay with a zero equilibrium stress model using a least-square technique are presented in Table 6. The R^2 of the emulsion systems was in the range 0.7011–0.9989, with 63.64 % of the systems exhibiting $R^2 > 0.9000$. The relatively high R^2 indicated that the model could be effectively used to describe the time-dependent data of the STASOL-stabilised emulsions. The presence of initial stress in the emulsion systems, as described by the first-order stress decay with a zero equilibrium stress model, confirmed that all emulsions were thixotropic and time-dependent in nature. All emulsions required stress to initiate flow. The rate of breakdown of the emulsions (k) reported in this study deviated from the reports of Razavi et al. (2008) who reported an increase in the rate of breakdown (k) of sesame paste with increasing shear rate and stabiliser concentration. Higher values of the model parameters of the first-order stress decay with a zero equilibrium stress (τ_o = 9.22–193.99 Pa and k = 1.39–3.90 s^{-1}) were reported for oil-in-water BGN flour-stabilised emulsions by Adeyi et al. (2016). The application of higher stress in food production translates to more energy required for the process.

Higher values of initial stress (τ_o) and comparable values of the rate of breakdown of the emulsions (k) were reported for emulsions stabilised with Balangu seed-derived hydrocolloid (Razavi & Karazhiyan, 2009). This suggested that a higher stress would be required to initiate flow in these systems than in STASOL-stabilised emulsions. This suggests that the production and processing of STASOL-stabilised emulsions would be more economic in comparison.

3.4.2.2. Weltman model. The model parameters of the Weltman model were evaluated as a function of STASOL, orange oil and water (Table 4). The Weltman model characterises the thixotropic and anti-thixotropic behaviour of foods. The R^2 of the Weltman model were in the range 0.6692–0.8862, with 81.82 % of the systems exhibiting $R^2 > 0.7716$. This made the Weltman model appropriate for describing the time-dependent behaviour of STASOL-stabilised emulsions.

In the Weltman model, the parameter A represents the initial shear stress of emulsions and was observed to be lowest in the emulsion (Run 3 (8:36:56 STASOL:oil:water)) with the lowest STASOL concentration indicating that flow was easier in relatively dilute systems. Run 2

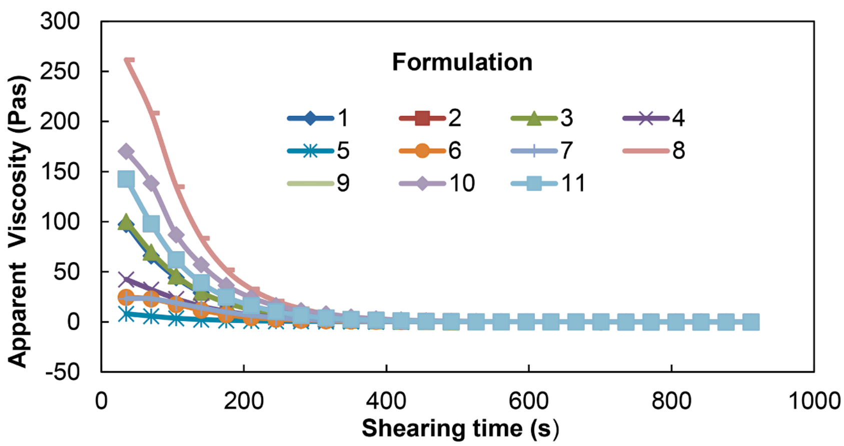

Fig. 4. Apparent viscosity vs shearing time of Bambara groundnut starch-soluble dietary fibre nanocomposite (STASOL)-stabilised emulsion.

Table 6
First-order stress decay with a zero equilibrium stress value and Weltman models for STASOL-stabilised emulsions.

				First-order stress decay with a zero equilibrium stress value			Weltman model		
Formulation	STASOL (%)	Orange oil (%)	Water (%)	τ_o (Pa)	k x 10^{-3}	R^2	A (Pa)	-B (Pa)	R^2
1	8	42	50	15.07 ± 0.12	13.76 ± 1.20	0.9897	14.23 ± 2.40	−2.229 ± 0.46	0.7749
2	20	30	50	15.11 ± 0.75	19.89 ± 2.78	0.9989	27.81 ± 1.31	−4.309 ± 0.85	0.8438
3	8	36	56	7.74 ± 1.24	11.87 ± 0.96	0.9901	8.12 ± 2.13	−1.261 ± 1.98	0.7964
4	10	38	62	22.51 ± 0.72	9.63 ± 0.52	0.9953	9.99 ± 0.42	−1.989 ± 0.64	0.6692
5	8	42	50	13.56 ± 0.60	15.43 ± 1.95	0.9626	11.29 ± 3.15	−1.746 ± 0.56	0.7331
6	8	30	62	6.63 ± 1.47	5.52 ± 0.39	0.8772	10.98 ± 3.01	−1.630 ± 0.97	0.8862
7	10	32	58	10.39 ± 0.58	8.61 ± 0.17	0.8790	12.75 ± 4.26	−1.899 ± 2.29	0.7948
8	14	30	56	20.87 ± 1.44	9.78 ± 0.56	0.9784	24.63 ± 1.51	−3.772 ± 1.65	0.8121
9	14	36	50	17.22 ± 2.85	8.61 ± 0.19	0.9029	20.73 ± 5.15	−3.083 ± 0.49	0.7717
10	12	34	54	12.34 ± 1.98	3.54 ± 0.08	0.7011	22.77 ± 2.17	−3.201 ± 0.33	0.8059
11	20	30	50	16.72 ± 0.89	7.39 ± 1.98	0.8416	21.70 ± 2.14	−3.177 ± 0.52	0.7850

STASOL: Bambara groundnut starch-soluble dietary fibre nanocomposite. Values are ± standard deviation. τ_o: Initial stress value. k: Rate of breakdown. A and B are constants. A: Initial shear stress. B: Thixotropic or anti-thixotropic behaviour. R^2: Coefficient of determination.

(20:30:50 STASOL:oil:water), with the highest STASOL concentration, had the highest A parameter value meaning that a larger stress was required to initiate the flow of the relatively viscous system. This was in agreement with the first-order stress decay with a zero equilibrium stress model (Section 3.4.2.1).

The model parameter B represents the time coefficient of thixotropic or anti-thixotropic behaviour of emulsions and gives information on the rate of breakdown of their thixotropic structure (Koocheki et al., 2009). A negative B value indicates thixotropic behaviour while a positive B value represents anti-thixotropic behaviour (Abu-Jdayil et al., 2004). The model parameter B was negative meaning all emulsions were thixotropic, therefore would become less viscous when subjected to an applied stress. The B parameter was closer to zero for emulsions with low STASOL concentrations and highest in the emulsion stabilised with the highest STASOL concentration. The value of the B parameter increases with solid content as the network needs a longer time to recover post shearing (Abu-Jdayil & Al-Omari, 2013).

The Weltman model has been reported as suitable for describing time-dependent rheological behaviour of food products such as semi-solid dairy desserts (Tarrega et al., 2004), mayonnaise (Singla et al., 2013), pistachio butter (Razavi et al., 2010) and BGN flour stabilised emulsions (Adeyi et al., 2016). Higher values of Weltman model parameters (A = 376.43–2213.49 Pa and B = 21.62–235.20 Pa) were reported for pistachio butter by Razavi et al. (2010). This indicated that a higher initial stress had to be exerted to induce the flow of pistachio butter compared to STASOL-stabilised emulsions. The positive B values reported suggested that the system exhibited anti-thixotropic behaviour. Singla et al. (2013) reported Weltman model parameters for mayonnaise as A = 5.05–5.11 Pa and B = 0.0005–0.0007 Pa. This means that less stress was required for the mayonnaise to flow than STASOL-stabilised emulsions. The B parameter values close to zero indicated that the apparent viscosity of mayonnaise was independent of time, meaning the system was neither thixotropic nor anti-thixotropic (Abu-Jdayil & Al-Omari, 2013).

3.4.2.3. Comparison of rheological models. The study conducted a comparative analysis between the first-order stress decay with a zero equilibrium stress value model and the Weltman model for modelling the time-dependent rheological properties of STASOL-stabilised emulsions. The evaluation was based on the statistical indicator R^2, where higher R^2 values indicate better model performance, as highlighted by Adeyi et al. (2021). Table 4 presents the results of this comparison. Both models performed well, but the first-order stress decay model with a zero equilibrium stress value exhibited slightly higher R^2 values across all emulsion formulations compared to the Weltman model. This suggests a better performance by the former model in capturing the rheological properties of the emulsions.

4. Conclusion

This study successfully optimised the emulsion stability of STASOL-stabilised emulsions by evaluating the influence of emulsion components (STASOL, orange oil, and water) and their ratios on their time-dependent rheological properties. All formulations demonstrated time-dependent shear-thinning behaviour under constant shear rate, with first-order stress decay and zero-equilibrium stress values, further confirming their thixotropic nature. Each emulsion system exhibited yield stress, indicating a threshold below which flow does not occur. Notably, the formulation with the highest STASOL concentration (20 %), the lowest orange oil content (30 %) and the lowest water content (50 %) exhibited the highest BSAVO and the lowest TSI, signifying optimal stability. Thus, it was concluded that increasing STASOL concentration while concurrently reducing orange oil and water concentrations enhances emulsion stability. This research highlights the viability of utilising natural biopolymer nanocomposites as emulsifiers in food products, offering an innovative approach to formulating stable emulsions in the food industry.

Funding details

Open access funding provided by the Cape Peninsula University of Technology.

CRediT authorship contribution statement

Yvonne Maphosa: Writing – original draft, Methodology, Investigation, Formal analysis, Conceptualization. **Oladayo Adeyi:** Writing – review & editing, Software, Formal analysis, Data curation. **Daniel Imwansi Ikhu-Omoregbe:** Supervision, Resources. **Victoria A. Jideani:** Writing – review & editing, Supervision, Resources, Funding acquisition, Data curation, Conceptualization.

Declaration of competing interest

The authors declare that they have no known competing financial interests or personal relationships that could have appeared to influence the work reported in this paper.

References

Abu-Jdayil, B., Banat, F., Jumah, R., Al-Asheh, S., Hammad, S., 2004. A comparative study of rheological characteristics of tomato paste and tomato powder solutions. Int. J. Food Prop. 7, 483–497. https://doi.org/10.1081/JFP-200032940.
Abu-Jdayil, B., Al-Omari, S.A., 2013. Rheological behavior of bentonite-polyester dispersions. Mech. Compos. Mater. 49, 277–284. https://doi.org/10.1007/s11029-013-9344-4.
Adeyi, O., Ikhu-Omoregbe, D., Jideani, V., 2014a. Emulsion stability and steady shear characteristics of concentrated oil-in-water emulsion stabilized by gelatinized

Bambara groundnut flour. Asian J. Chem. 26, 4995–5002. https://doi.org/10.14233/ajchem.2014.16287.

Adeyi, O., Ikhu-Omoregbe, D., Jideani, V., 2014b. Modelling the time-dependent rheological properties of oil- in-water emulsions stabilized with gelatinized Bambara groundnut flour. LAUTECH J. Eng. Technol. 10, 1–11.

Adeyi, O., Ikhu-Omoregbe, D., Jideani, V., 2016. Effect of sodium chloride salt on the rheological properties of sunflower oil-in-water emulsion stabilized by gelatinized Bambara groundnut flour. LAUTECH J. Eng. Technol. 10, 55–64.

Adeyi, A.J., Adeyi, O., Oke, E.O., Olalere, O.A., Oyelami, S., Ogunsola, A.D., 2021. Effect of varied fiber alkali treatments on the tensile strength of *Ampelocissus cavicaulis* reinforced polyester composites: prediction, optimization, uncertainty and sensitivity analysis. Adv. Ind. Eng. Polym. Res. 4, 29–40. https://doi.org/10.1016/j.aiepr.2020.12.002.

Adeyi, O., Adeyi, A.J., Oke, E.O., Okolo, B.I., Olalere, O.A., Taiwo, A.E., Aremu, O.S., Qwebani-Ogunleye, T., Maphosa, Y., Ogunsola, A.D., 2022. Heat-assisted extraction of phenolic-rich bioactive antioxidants from *Enantia chlorantha* stem bark: multi-objective optimization, integrated process techno-economics and profitability risk assessment. SN Appl. Sci. 5, 153. https://doi.org/10.1007/s42452-023-05372-1.

Akbari, S., Nour, A.H., 2018. Emulsion types, stability mechanisms and rheology: a review. Int. J. Innov. Res. Sci. Stud. 1, 11–17. https://doi.org/10.53894/ijirss.v1i1.4.

Alanzi, H., Alenezi, H., Adeyi, O., Adeyi, A.J., Olusola, E., Gan, C.Y., Olalere, O.A., 2024. Process optimization, multi-gene genetic programming modeling and reliability assessment of bioactive extracts recovery from *Phyllantus emblica*. J. Eng. Res. https://doi.org/10.1016/j.jer.2024.02.020.

Alvarez, D., Barbut, S., 2013. Effect of inulin, β-glucan and their mixtures on emulsion stability, color and textural parameters of cooked meat batters. Meat Sci. 94, 320–327. https://doi.org/10.1016/j.meatsci.2013.02.011.

Arrebola, I.N., Billon, L., Aguirre, G., 2021. Microgels self-assembly at liquid/liquid interface as stabilizers of emulsion: past, present & future. Adv. Colloid Interface Sci. 287, 102333. https://doi.org/10.1016/j.cis.2020.102333.

Blasi, M., Algieri, C., Chakraborty, S., Calabrò, V., 2023. Application of Turbiscan stability index for the preparation of alumina photocatalytic membranes for dye removal. Membranes 13, 400. https://doi.org/10.3390/membranes13040400 (Basel).

Chen, Y., Chen, Y., Jiang, L., Yang, Z., Fang, Y., Zhang, W., 2023. Shear emulsification condition strategy impact high internal phase Pickering emulsions stabilized by coconut globulin-tannic acid: structure of protein at the oil-water interface. LWT 187, 115283. https://doi.org/10.1016/j.lwt.2023.115283.

Choi, S.J., Won, J.W., Park, K.M., Chang, P.-S., 2014. A new method for determining the emulsion stability index by backscattering light detection. J. Food Process Eng. 37, 229–236. https://doi.org/10.1111/jfpe.12078.

Fagundes, F.M., Santos, N.B.C., Damasceno, J.J.R., Arouca, F.O., 2018. Study on the stability of a shear-thinning suspension used in oil well drilling. Oil Gas Sci. Technol. Rev. IFP Energies nouvelles 73, 1–6. https://doi.org/10.2516/ogst/2018007.

Farahmandfar, R., Salahi, M.R., Asnaashari, M., 2019. Flow behavior, thixotropy, and dynamic viscoelasticity of ethanolic purified basil (*Ocimum bacilicum* L.) seed gum solutions during thermal treatment. Food Sci. Nutr. 7 (5), 1623–1633.

Ghica, M.V., Hirjau, M., Lupuleasa, D., Dinu-Pirvu, C.E., 2016. Flow and thixotropic parameters for rheological characterization of hydrogels. Molecules 21, 786–803. https://doi.org/10.3390/molecules21060786.

Huang, Y., Gilmour, S.G., Mylona, K., Goos, P., 2019. Optimal design of experiments for non-linear response surface models. J. R. Stat. Soc. Ser. C Appl. Stat. 68, 623–640. https://doi.org/10.1111/rssc.12313.

IBM, 2016. Statistical package for the social science. IBM SPSS - IBM Analytics. IBM SPSS Software.

Junqueira, L.A., Amaral, T.N., Oliveira, N.L., Prado, M.E.T., de Resende, J.V., 2018. Rheological behavior and stability of emulsions obtained from Pereskia aculeata Miller via different drying methods. Int. J. Food Prop. 21, 21–35. https://doi.org/10.1080/10942912.2018.1437177.

Kakran, M., Antipina, M.N., 2014. Emulsion-based techniques for encapsulation in biomedicine, food and personal care. Curr. Opin. Pharmacol. 18, 47–55. https://doi.org/10.1016/j.coph.2014.09.003.

Koocheki, A., Ghandi, A., Razavi, S.M.A., Mortazavi, S.A., Vasiljevic, T., 2009. The rheological properties of ketchup as a function of different hydrocolloids and temperature. Int. J. Food Sci. Technol. 44, 596–602. https://doi.org/10.1111/j.1365-2621.2008.01868.x.

Kupikowska-Stobba, B., Domagała, J., Kasprzak, M.M., 2024. Critical review of techniques for food emulsion characterization. Appl. Sci. 14, 1069. https://doi.org/10.3390/app14031069.

Lamidi, S., Olaleye, N., Bankole, Y., Obalola, A., Aribike, E., Adigun, I., 2023. Applications of response surface methodology (RSM) in product design, development, and process optimization. IntechOpen. https://doi.org/10.5772/intechopen.106763.

Li, Z., Huang, X., Xu, X., Bai, Y., Zou, C., 2024. Unstable coalescence mechanism and influencing factors of heterogeneous oil droplets. Molecules 29, 1582. https://doi.org/10.3390/molecules29071582.

Liu, Y., Chen, W., Chen, C., Zhang, J., 2015. Physicochemical property of starch-soluble dietary fiber conjugates and their resistance to enzymatic hydrolysis. Int. J. Food Prop. 18, 2457–2471. https://doi.org/10.1080/10942912.2014.968785.

Liu, F., He, W., Huang, X., Yin, J., Nie, S., 2024. The emulsification and stabilization mechanism of an oil-in-water emulsion constructed from tremella polysaccharide and citrus pectin. Foods 13, 1545. https://doi.org/10.3390/foods13101545.

Luo, M., Qi, X., Ren, T., Huang, Y., Keller, A.A., Wang, H., Wu, B., Jin, H., Li, F., 2017. Heteroaggregation of CeO2 and TiO2 engineered nanoparticles in the aqueous phase: application of turbiscan stability index and fluorescence excitation-emission matrix (EEM) spectra. Colloids Surf. A Physicochem. Eng. Asp. 533, 9–19. https://doi.org/10.1016/j.colsurfa.2017.08.014.

Maphosa, Y., Jideani, V.A., Adeyi, O., 2017. Effect of soluble dietary fibres from Bambara groundnut varieties on the stability of orange oil beverage emulsion. Afr. J. Sci. Technol. Innov. Dev. 9, 69–76. https://doi.org/10.1080/20421338.2016.1263436.

Maphosa, Y., Jideani, V.A., 2018. Factors affecting the stability of emulsions stabilised by biopolymers. In: Karakuş, S. (Ed.), Science and Technology Behind Nanoemulsions. IntechOpen. https://doi.org/10.5772/intechopen.75308.

Maphosa, Y., Jideani, V.A., Ikhu-Omoregbe, D.I., 2022a. *Vigna Subterranea* (L.) Verdc starch-soluble dietary fibre potential nanocomposite: thermal behaviour, morphology and crystallinity. Processes 10, 299. https://doi.org/10.3390/pr10020299.

Maphosa, Y., Jideani, V.A., Ikhu-Omoregbe, D.I., 2022b. Novel *Vigna subterranea* (L.) Verdc soluble dietary fibre-starch nanocomposite: functional and antioxidant characteristics. Food Technol. Biotech. 60, 361–374. https://doi.org/10.17113/ftb.60.03.22.7409.

Maphosa, Y., Ikhu-Omoregbe, D.I., Adeyi, O., Jideani, V.A., 2023. Effect of storage time and temperature on the stability and rheological properties of starch-soluble dietary fiber nanocomposite stabilized emulsion. Chem. Eng. Commun. 211, 546–558. https://doi.org/10.1080/00986445.2023.2261099.

Ng, S.P., Khor, Y.P., Lim, H.K., Lai, O.M., Wang, Y., Wang, Y., Cheong, L.Z., Arbi Nehdi, I., Mansour, L., Tan, C.P., 2020. Fabrication of concentrated palm olein-based diacylglycerol oil-soybean oil blend oil-in-water emulsion: in-depth study of the rheological properties and storage stability. Foods 9, 877. https://doi.org/10.3390/foods9070877.

Oke, E.O., Okolo, B.I., Adeyi, O., Adeyi, J.A., Otolorin, J.A., Nnabodo, D., Ude, C.J., Okhale, S.E., Adeyanju, J.A., Adeniyi, A.G., Eleanyan, E., Agbai, S.O., 2023. Bioactive extract production from *Citrullus colocynthis* fruit via microwave-assisted extraction: experimental optimization, process design and economics with uncertainty quantification. J. Pharm. Innov. 18, 687–703. https://doi.org/10.1007/s12247-022-09676-4.

Oliveira, T.F., Cunha, F.R., 2015. Emulsion rheology for steady and oscillatory shear flows at moderate and high viscosity ratio. Rheol. Acta 54, 951–971. https://doi.org/10.1007/s00397-015-0885-4.

Perez-Mosqueda, L., Trujillo-Cayado, L.A., Carrillo, F., Ramirez, P., 2015. Formulation and optimization by experimental design of eco-friendly emulsions based on D-limonene. Colloids Surf. B Biointerfaces 128, 127–131. https://doi.org/10.1016/j.colsurfb.2015.02.030.

Rahayu, W.D., Syafitri, U.D., Soleh, A.M., 2019. D-optimal design for ordinal responses in mixture experiments. J. Phys. Conf. Ser. 1317, 012017. https://doi.org/10.1088/1742-6596/1317/1/012017.

Razavi, S.M.A., Karazhiyan, H., 2009. Flow properties and thixotropy of selected hydrocolloids: experimental and modeling studies. Food Hydrocoll. 23, 908–912. https://doi.org/10.1016/j.foodhyd.2008.05.010.

Razavi, S.M.A., Habibi, N.M.B., Alaee, Z., 2008. Rheological characterization of low fat sesame paste blended with date syrup. Int. J. Food Prop. 11, 92–101. https://doi.org/10.1080/10942910701233397.

Razavi, S.M.A., Taghizadeh, M., Ardekani, A.S., 2010. Modeling the time-dependent rheological properties of pistachio butter. J. Nuts Relat. Sci. 1, 38–45. https://doi.org/10.22034/JON.2010.515765.

Schilling, J., Schmid, J., 2024. Comprehensive rheological analysis of structurally related acetan-like heteroexopolysaccharides from two *Kozakia baliensis* strains in surfactants and galactomannan blends. New Biotechnol. 82, 75–84. https://doi.org/10.1016/j.nbt.2024.05.003.

Singla, N., Verma, P., Ghoshal, G., Basu, S., 2013. Steady state and time dependent rheological behaviour of mayonnaise (egg and eggless). Int. Food Res. J. 20, 191–199.

Tarrega, A., Duran, L., Castell, E., 2004. Flow behavior of semi-solid dairy desserts: effect of temperature. Int. Dairy J. 14, 345–353. https://doi.org/10.1016/j.idairyj.2003.12.004.

Trujillo-Cayado, L.A., Alfaro, M.C., Muñoz, J., Raymundo, A., Sousa, I., 2016. Development and rheological properties of ecological emulsions formulated with a biosolvent and two microbial polysaccharides. Colloids Surf. B Biointerfaces 141, 53–58. https://doi.org/10.1016/j.colsurfb.2015.11.046.

Yin, B., Zhang, R., Yao, P., 2015. Influence of pea protein aggregates on the structure and stability of pea protein/soybean polysaccharide complex emulsions. Molecules 20, 5165–5183. https://doi.org/10.3390/molecules20035165.

Zalewska, A., Kowalik, J., Grubecki, I., 2019. Application of Turbiscan lab to study the effect of emulsifier content on the stability of plant origin dispersion. Chem. Process Eng. 40, 399–409. https://doi.org/10.24425/cpe.2019.130214.

Zhang, H., Yang, H., Wang, F., Zhao, H., Li, X., Zhou, B., Zhang, M., Kang, W., Sarsenbekuly, B., Aidarova, S., Gabdullin, M., 2020. Study on the stabilization of emulsion formed by two different inclusion complexes. Colloids Surf. A Physicochem. Eng. Asp. 594, 124651. https://doi.org/10.1016/j.colsurfa.2020.124651.